Insights into the structural characteristics and in vitro starch digestibility on parboiled rice as affected by ultrasound treatment in soaking process

Alia Shah, Yunchun Wang, Han Tao [*], Wencheng Zhang [*], Shuqing Cao [*]

Engineering Research Center of Bio-Process of Ministry of Education, School of Food and Biological Engineering, Hefei University of Technology, Hefei, China

A B S T R A C T

This study investigated ultrasound treatment as a protective parboiling technology for producing low GI rice. Indica and Japonica rice with different amylose contents were subjected to different ultrasound times (15 min, 30 min, and 60 min) and amplitudes (30, 60, and 100%) under soaking conditions for parboiling applications. Starch granules merged and lost their shape when ultrasound treatment time and amplitudes were increased up to 15 min and 30%, respectively. It increased the crystallinity, gelatinization temperatures and decreased pasting viscosity, promoting more resistant starch. The predicted glycemic index (GI) was reduced from 62.9 and 57.6 to 51.3 and 47.1 for Japonica and Indica, respectively. These results suggested that ultrasound soaking is a promising physical method to produce parboiled rice with a lower GI by promoting the formation of amylose chains and decreasing enzyme penetration efficiency.

1. Introduction

Rice plays a vital role as a staple food and serves as a primary source of nutrition for over half of the global population. The consumption of rice, especially refined rice, leads to rapid digestion, resulting in a high glycemic index (GI) with a rapid spike in blood sugar levels (Flores-Silva et al., 2017). GI is commonly classified into 3 main groups: low ($\leq$55), medium (56 $\leq$ 69), and high ($\geq$70) GI, which is associated with an elevated risk of developing type-2 diabetes and cardiovascular diseases (Venn & Green 2007). Food production process, rice variety, amylose/amylopectin ratio, and the presence of other chemical compositions contributes the different GI (Zhang et al., 2019). High-amylose rice exhibits lower blood glucose levels and slower emptying of human gastrointestinal tract compared to those with low levels of amylose (Liu et al., 2020). Therefore, a lot of technologies are used to meet the requirements of various consumers including chronic disease patients and diabetes people by modifying the structure or molecular organization of starch molecules through chemical (Cai et al., 2020), physical (Zou et al., 2020), or enzymatic methods (Gui et al., 2022). Especially, physical approaches are considered the most suitable due to their simplicity and safety (Zia-ud-Din et al., 2017).

Ultrasound has been widely used to promote food morphology and structural characteristics by high shear and mechanical energy to produce acoustic streaming within a liquid (Li et al., 2021b). The previous studies found that ultrasound treatment showed different trend on starch granules depending on the intensity and time. High-intensity ultrasound, characterized with amplitudes from 20 to 100 kHz, creates strong shear forces, high temperature, and free radicals, changing rice grain structure and function (Kaur & Gill 2019, Vela et al., 2021). Ultrasound treated starch displayed an increased crystallinity, higher swelling power and water absorption capacity (Kunyanee & Luangsakul 2020, Liang et al., 2021). Meanwhile, lower ultrasound characterized by small acoustic amplitudes (>1 kHz), brings non-thermal effects on the granules by altering the morphological characteristics (Kentish et al., 2014). Ultrasonic waves cause many voids and cracks in the starch granules with fragmented chains from amylopectin (Lu et al., 2018), enhances the extraction of phenolic compounds, polysaccharides and improved the antioxidant activity (Estivi et al., 2022). These studies suggest that ultrasound treatment has the potential to change the physicochemical properties of rice grains.

Parboiling refers to a hydrothermal procedure in which kernels are soaked (above 58 °C), heated (120 °C), and dried before de-husking (Sittipod & Shi 2016). Soaking, as the first step, makes the paddy immersed in water for 2 or 3 days to arrive at optimum hydration. The moisture, temperature, and processing period during soaking treatment is critical to the product quality which is traditionally divided into room-temperature soaking and high-temperature soaking treatments. Room-temperature soaking takes from 1 to 3 days for hydration equilibration

---

while the high-temperature soaking takes 5 h in hot water. The long and hydrothermal conditions usually results in an unpleasant odor, lower tenderness, excessive water absorption and hull splitting and taste due to microbial activities and changed paddy structure (Lamberts et al., 2008, Thammapat et al., 2016). The processing-induced worse edible and nutritional quality of rice is necessary to be improved by new technology application. However, systematic studies on the dual application of ultrasound and soaking treatments on the parboiled rice quality are limited. It is unknown how the presence of ultrasonic action affects the exterior structure and digestibility of rice. Thus, this study intends to investigate the improvement of ultrasound-assisted soaking on the structural, thermal, and digestion properties of parboiled rice and provide valuable insights into the potential use of ultrasound as a method for producing low glycemic index rice.

2. Materials and methods

2.1. Materials

Indica and Japonica paddy cultivars with different amylose contents were obtained from Expert Seed Private Ltd, China. Amyloglucosidase (Cat No. J10032. Conc. 3300 U/MI), α amylase (Cat No. A3176-1MU. Conc. 3000 U/g), and Glucose oxidase/peroxidase (GODPOD) assay kit are perchased from Sigma-Aldrich Chemical Co. LLC (Santa Clara, USA) and Megazyme International China Ltd. All reagents were of analytical grade.

2.2. Ultrasound-assisted soaking and parboiling treatment

Paddy (500 g) was subjected to an ultrasound-assisted soaking treatment in water (1.5 L) (model: JY98-IIIDN, Kerui Instruments Co., Ltd, China). The ultrasound-assisted soaking treatment in the study was performed using a specific set of conditions. The rice samples subjected to ultrasound-assisted soaking treatment recorded a temperature ranging from 20 to 25 °C with a power of 1200 W. The ultrasound-assisted soaking time was set over a range of 15 min, 30 min, and 60 min, while the amplitude was adjusted over a range of 30%, 60%, and 100%. Steaming the paddy for 10 min at 110 °C was chosen to achieve the desired fresh parboiled rice. Then, the parboiled rice was dried in an oven (CREF-5013B from Kerui Instruments Co., Ltd. Dongguan, China) at 40 °C until it reached a consistent moisture content (11 ± 1%) for Indica rice and (12 ± 1%) for Japonica rice (wet basis). Then, the parboiled rice samples were dehulled using a huller (HD8888 from AUYAS, Yantai, China) and ground into powder using an electric blender (DL0MD18, Dong Lim Co., Guangdong, China), then passed through an 80-mesh sieve for the following analysis. In the following discussion, the term "native" refers to untreated raw rice.

For traditional parboiled rice, 500 g paddy was soaked in water (1.5 L) at 60 °C for 4 h, and then done by heating, and drying process as the same as described above.

2.3. Scanning electron microscopy (SEM)

Rice micro structural changes were observed by a scanning electron microscope (Model: Regulus 8230 from Hitachi, Ltd., Japan) with a high-resolution field emission source. The rice grains were manually cleaved, set up on an aluminum stud with a thin layer of gold using a sputter coater and observed under the voltage of 2.0 kV and a magnification of × 250.

2.4. Protein and amylose content determination

The protein and apparent amylose contents of rice sample was individually determined by (AOAC 2002) and (Peng et al., 2021) respectively.

2.5. Fourier transforms infrared spectroscopy (FTIR)

The FTIR spectra of rice were collected using a Nicolet 5700 spectrometer manufactured by Thermo Nicolet Co. (Waltham USA). The sample was prepared by mixing 1 mg of rice powder with 100 mg of KBr, then pressed into round tablets and scanned in the range of 4000–400 cm^{-1} with a resolution of 4 cm^{-1} according to (Yang et al., 2020).

2.6. X-ray diffraction (XRD)

The XRD crystalline spectra of rice were collected by a fixed target X-ray diffractometer (PANalytical B.V., Almelo, Holland). The XRD analysis was conducted at 40 mA and a voltage of 40 kV, using Cu Kα radiation with a wavelength of 1.54 nm. The rice samples were scanned from 5° to 40°.The relative crystallinity (RC) of samples was measured according to (Tao et al., 2021).

2.7. Thermal properties

The gelatinization characteristics of rice were determined using a Q200 DSC (TA Instruments, Delaware, USA). The rice samples 3 mg along with 9 μL of distilled water were accurately weighed in an aluminum pan, sealed, and stored for 24 h at 4 °C to reach equilibrium. The samples were scanned from 20 to 120 °C at an average heating rate of 10 °C/min. The gelatinization enthalpy (ΔH), peak (T_p), onset (T_o), and conclusion temperatures (T_c) were measured from the heating curve.

2.8. Pasting properties

The pasting characteristics of rice were analyzed using a FDV-E Economical Starch Rapid Visco Analyzer (model Nirun Co. Ltd., Shanghai), according to (Sowbhagya & Bhattacharya 2001) with minor modifications. Rice powder (0.8 g) was dispersed in distilled water in an aluminum canister to prepare rice slurry (8%, w/v). The program condition is set as heating from 30 to 95 °C, holding at 95 °C for 30 min, and decreasing to 50 °C. The speed and heating/cooling rate for thorough dispersion was 75 rpm/min and 3 °C/min respectively.

2.9. Resistant starch determination (RS)

RS of rice samples was measured according to (Flores-Silva et al., 2017). Samples of 100 mg were weighed and incubated at 37 °C in a 4 mL of 0.1 M sodium maleate buffer (pH 6.0) with AMG (3.3 U/mL) and α-amylase (10 mg/mL) solution for 16 h. Then, 4 mL of ethanol was added to the solution, followed by centrifugation at 1500 *g* for 10 min to obtain the RS pellet. The above step was repeated twice. Then, 2 M KOH was added to the RS pellet, and stirred magnetically in iced water. Subsequently, the solution was incubated for 30 min at 50 °C with AMG (amyloglucosidase). D-glucose content, which was measure of the RS in the samples, was measured using the GOPOD. Digestible starch (DS) content was determined by pooling the original supernatant and the washings and measured D-glucose content with GOPOD. Total starch (TS) was calculated as the sum of DS and RS, providing an overall assessment of the starch content in the rice samples.

2.10. In vitro glycemic index (GI)

The GI of samples was evaluated according to the method developed by (Englyst et al., 1992). Rice powder (100 mg) was dispersed with 4 mL sodium maleate solution (0.1 M, pH 6.0) contained α-amylase (10 mg/mL) and AMG (3.3 U/mL). The mixture was continuously stirred at speed of 150 rpm/min at 37 °C in a water bath. 0.5 mL aliquots were taken from the mixture at 0, 30, 60, 120, 150, and 180 min intervals and were mixed with ethanol (4 mL) to stop the digestion, followed by centrifugation for 10 min at 1500 *g*. The supernatant obtained after

centrifugation was subjected to glucose determination using a glucose oxidase–peroxidase (GOPOD) kit. To calculate hydrolysis Index, the area under the hydrolysis curve of the sample was divided by the area corresponding of a reference sample (white bread). The eGI was calculated according to (Goñi et al., 1997): eGI = 39.7+(0.549 HI).

Where eGI is the estimated glycemic index and HI represents the term "Hydrolysis Index." The Hydrolysis Index is a measure that indicates how rapidly a particular carbohydrate or food is broken down into glucose during digestion. In the context of calculating the estimated eGI, the HI value is used as a variable to determine the predicted glycemic index of a food item.

2.11. Texture profile analysis

Rice grain (10 g each) was put into water (100 mL) at 98 ± 1 °C. After 10 min, cooking time was start to measure every minute. For evaluating the cooking extent, 10 rice grains were pressed into two glass plates until the central white core disappeared (Tian et al., 2018). After cooked samples were cooled to 20 °C for 2 h, five full-length grains from each sample were subjected to a texture measurement using a TA-XT2i analyzer with a 36-mm cylindrical probe. The parameters were obtained at a 75% strain; pre-test speed, test speed and post-test speed were set as 2.0 mm/s, 1.0 mm/s, and 1.0 mm/s respectively. Five replications were performed for each sample.

2.12. Statistical analysis

All experiments mentioned in research were performed in triplicate. Statistical investigation was performed using Origin 2019 software (OriginLab Inc., USA) and Statistix. 8 (Analytical Software, Tallahassee, FL, USA) as mentioned. An analysis of variance was conducted, and the mean separation was analyzed using (ANOVA) and Tukey's test (P <
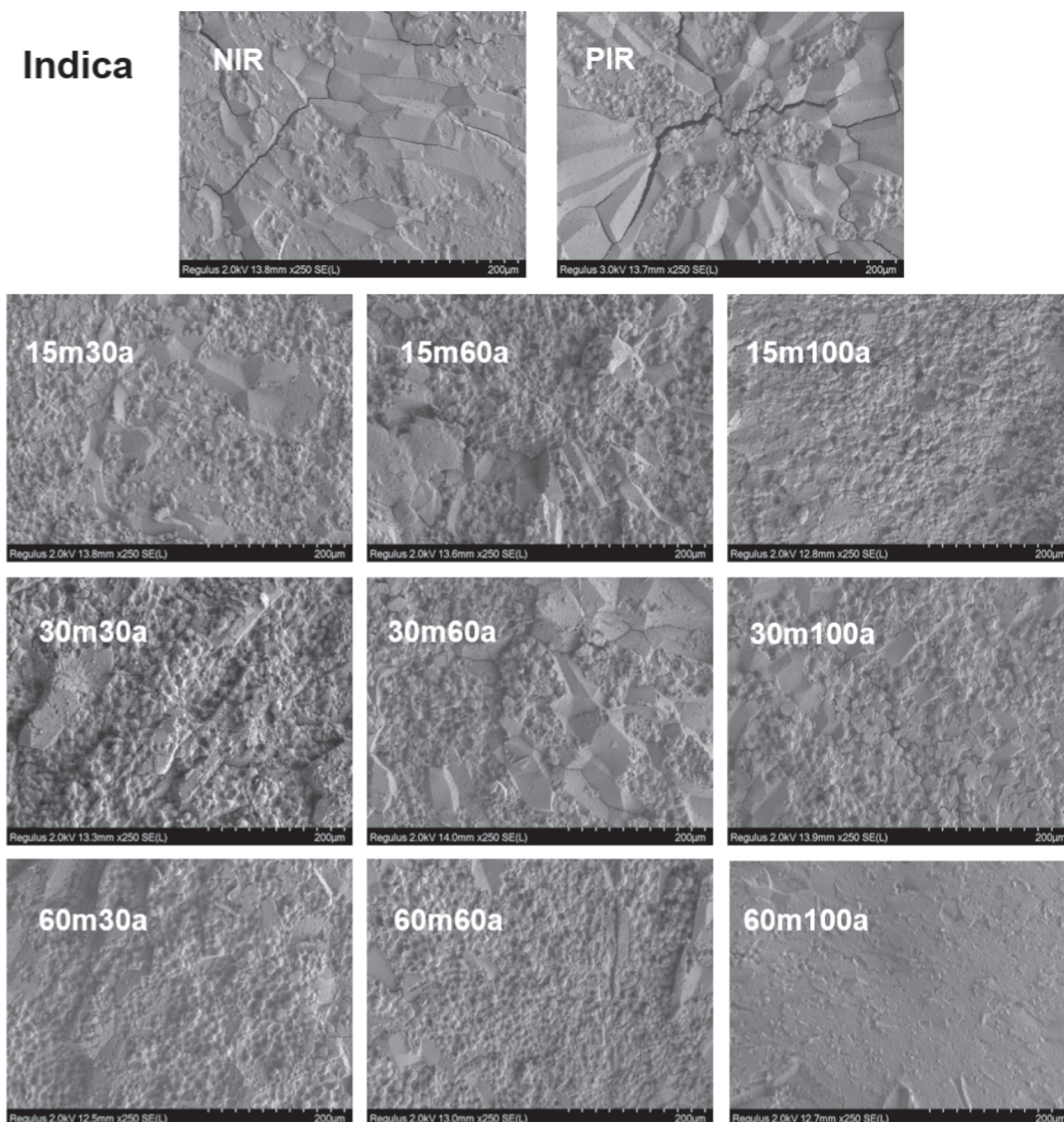

Fig. 1. SEM images of native, parboiled, and ultrasound-assisted parboiled Indica (A) and Japonica (B) rice cultivars under different times and amplitudes.
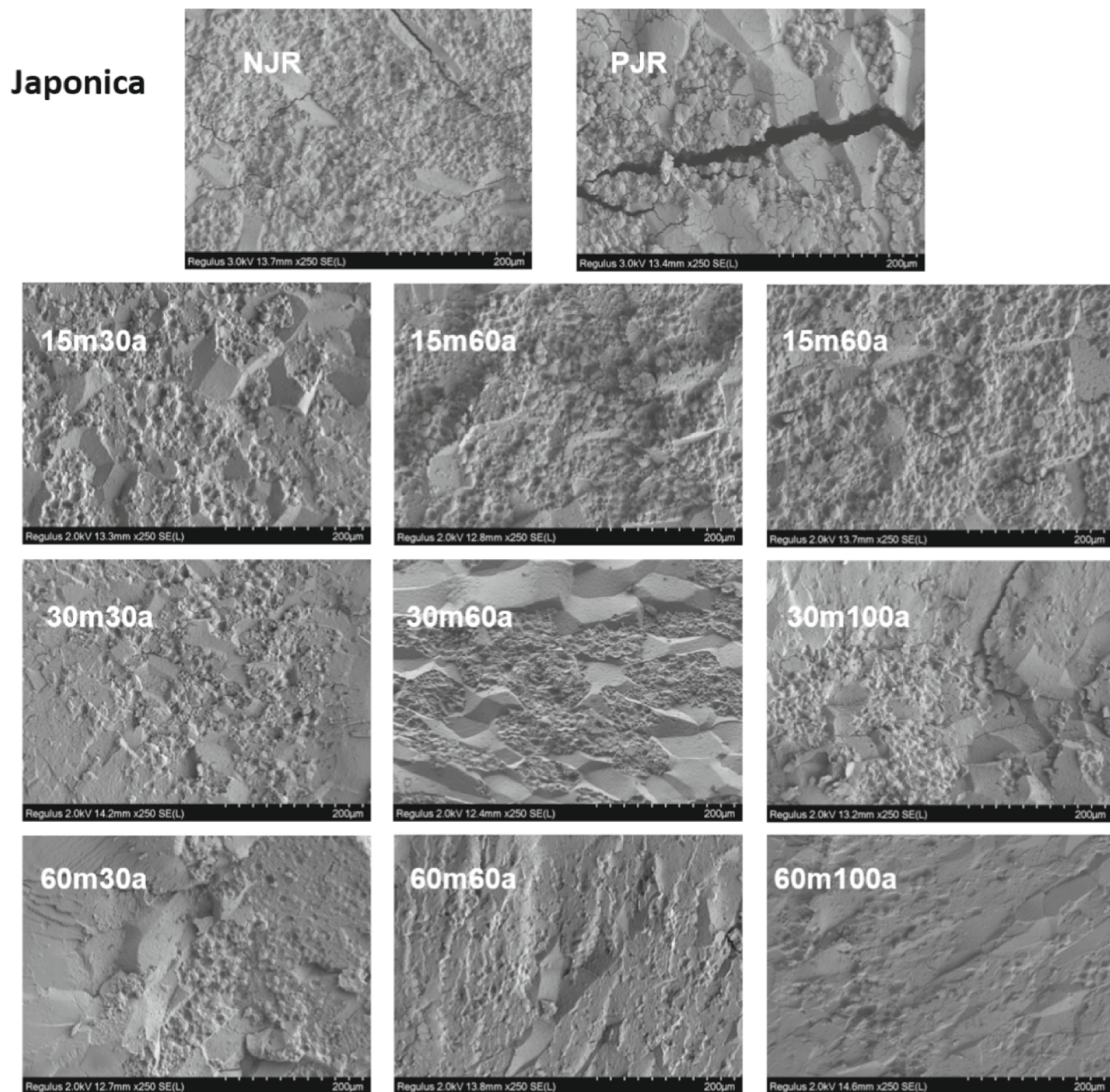
Fig. 1. (*continued*).

0.05).

3. Results and discussion

3.1. Grain surface microstructure

The cross-section of rice grains was observed by SEM. In Fig. 1A and 1B inter-granular spaces and cracks were observed on the outer peripheral surface of native and parboiled rice, exposing internal starch granules. After ultrasound-assisted parboiling treatment, the external fissure or cracks were no longer observed. Starch granules were increased in size, merged together, sealed up granular spaces, and tightly packed to form a smooth surface. More granules got slightly fused and lost their shape as the ultrasound time and amplitude increased. This change may have attributed to the debranching of amylopectin and rearrangement and alignment of starch chains caused by the action of ultrasound waves due to the acoustic streaming, shear force, and water penetration into starch granules that transformed random coils into the double helix structure (Cao et al., 2020, Kentish et al., 2014). The

collapsing cavitations bubbles near the surface membranes resulted in micro-fractures in ultrasound-treated potato starch (Nie et al., 2019). The micro-structural changes in parboiled rice induced by ultrasound treatment are primarily attributed to the physical activities generated by acoustic cavitations, including shock waves, microjets, microstreaming, turbulence, and water influence at the solid–liquid interface. These changes can result in alterations in the structural characteristics and properties of rice grains, which ultimately affect the quality and digestibility of rice.

3.2. Protein and amylose content analysis

The protein and amylose content of each sample is shown in Table. 1. Indica rice varieties exhibited relatively higher levels of protein. The difference between two cultivars in protein content is due to the different genotype characteristics. The proteins content was further increased by parboiling treatment due to the migration of proteins and minerals from the aleurone (outer) layer of the rice kernel into the endosperm during the parboiling process (Pal et al., 2018). As for the

Table 1

Total starch (TS), digestible starch (DS), resistant starch (RS), amylose (AC), and protein content (PC) in native, parboiled and ultrasound-assisted parboiled Indica and Japonica rice cultivars.

Cultivars	Time (min)	Amplitude (%)	TS(100/g)	DS(100/g)	RS (100/g)	AC (100/g)	PC (100/g)
Indica	Native	0	77.8 ± 1.2[a]	60.8 ± 0.3[a]	16.98 ± 0.5[d]	18.9 ± 0.3 [g]	8.4 ± 0.68[ab]
	IPR	0	77.2 ± 0.8[b]	58.0 ± 0.4[b]	19.2 ± 0.3[c]	20.1 ± 0.3[f]	9.1 ± 0.41[a]
	15	30	77.4 ± 0.4[ab]	57.3 ± 0.3[bc]	20.07 ± 0.4[c]	22.0 ± 0.3[e]	8.7 ± 0.28[a]
		60	77.4 ± 0.7[ab]	54.9 ± 0.9[d]	22.43 ± 0.3[b]	25.1 ± 0.2[bc]	8.9 ± 0.49[a]
		100	77.1 ± 1.3[b]	54.0 ± 0.1[d]	23.08 ± 0.1[b]	26.8 ± 0.3[b]	9.0 ± 0.63[a]
	30	30	77.3 ± 1.1[b]	55.8 ± 1.2[c]	21.41 ± 0.6[c]	24.3 ± 0.5[c]	9.2 ± 0.53[a]
		60	77.2 ± 0.9[b]	49.7 ± 0.5[f]	27.41 ± 0.5[a]	29.2 ± 0.4[a]	9.4 ± 0.27[a]
		100	77.2 ± 0.8[b]	50.4 ± 0.2[e]	26.74 ± 0.4[a]	28.2 ± 0.1[a]	9.4 ± 0.65[a]
	60	30	77.6 ± 0.6[a]	54.3 ± 0.2[d]	23.23 ± 0.5[b]	25.3 ± 0.2[bc]	9.1 ± 0.78[a]
		60	77.5 ± 0.5[a]	54.8 ± 0.7[d]	22.62 ± 0.7[b]	23.8 ± 0.5 [cd]	9.0 ± 0.48[a]
		100	77.1 ± 1.2[b]	56.3 ± 0.3[c]	20.73 ± 0.8[c]	21.7 ± 0.3[e]	9.3 ± 0.52[a]
Japonica	Native	0	80.5 ± 1.4[a]	71.8 ± 0.6[a]	7.32 ± 0.3[f]	8.6 ± 0.3[f]	5.7 ± 0.23[b]
	JPR	0	79.9 ± 1.1[b]	68.4 ± 0.7[a]	9.78 ± 0.5[e]	11.4 ± 0.4[e]	6.4 ± 0.47[a]
	15	30	80.2 ± 0.7[a]	66.6 ± 0.5[c]	13.57 ± 0.4[d]	15.6 ± 0.3[d]	5.7 ± 0.42[b]
		60	80.3 ± 1.2[a]	66.1 ± 0.3[c]	14.11 ± 0.3[c]	18.7 ± 0.5[b]	5.7 ± 0.38[b]
		100	80.1 ± 0.8[a]	65.5 ± 0.6[c]	14.51 ± 0.5[c]	17.0 ± 0.3[c]	5.9 ± 0.31[a]
	30	30	80.2 ± 0.8[a]	64.9 ± 0.4[c]	15.21 ± 0.3[b]	16.6 ± 0.2[d]	6.2 ± 0.51[a]
		60	79.6 ± 1.3[b]	61.5 ± 0.6[d]	18.04 ± 0.3[a]	21.4 ± 0.1[a]	6.4 ± 0.41[a]
		100	79.5 ± 1.1[b]	61.9 ± 0.3[d]	17.57 ± 0.6[a]	19.8 ± 0.2[b]	6.5 ± 0.68[a]
	60	30	79.3 ± 1.0[b]	65.2 ± 0.2[a]	14.09 ± 0.3[c]	17.2 ± 0.3[c]	6.6 ± 0.38[a]
		60	79.8 ± 0.7[b]	64.3 ± 0.6[b]	15.44 ± 0.5[b]	19.8 ± 0.2[b]	6.2 ± 0.29[a]
		100	79.4 ± 0.9[b]	64.3 ± 0.1[c]	15.05 ± 0.3[b]	18.2 ± 0.4[b]	5.9 ± 0.23[a]

amylose content, there is a lower value in Japonica rice than in Indica, but after ultrasound-assisted parboiling, it increased individually to 21.4 and 29.2 for Japonica and Indica rice, respectively. It could be ascribed to the degradation of the amylopectin side chain, leading to the release of long branch chains as amylose (Li et al., 2018). Ultrasonication can induce a phenomenon called acoustic cavitations resulting in physical degradation. (Yang et al., 2019) reported that acoustic cavitations led to the formation and collapse of microscopic bubbles in the liquid, evolving in the generation of pressures, free radicals, and shock waves. It could easily modify the granular structure and change its functional properties by attacking the amorphous region in starch (Morales-Trejo et al., 2022).

3.4. Fourier transforms infrared spectroscopy

FTIR (Fourier Transform Infrared) spectra were presented in Fig. 2A. It was observed that there were no significant changes in the FTIR spectra, indicating that the overall molecular structure of rice remained unchanged and ultrasound-assisted parboiling treatment did not induce any chemical changes in either rice cultivars. It was consistent with results from (Kunyanee & Luangsakul 2020) where the peaks at 3300 cm^{-1}, 2923 cm^{-1}, 1643 cm^{-1}, 1344 cm^{-1}, and 997 cm^{-1} indicated the presence of O—H, C—H, C—O, C—O—H, and to C—O—C groups, respectively. In contrast, the short crystalline pattern was modified when the parboiling treatment was applied, especially at 30 min of ultrasound treatment with amplitude of 60%. The absorbance ratio at 1047/1022 cm^{-1} an indicator of the short-range order, was increased from 0.872 to 0.94.4 for Indica rice and from 0.873 to 0.934 for Japonica rice, respectively (Kunyanee & Luangsakul 2020). This increase after ultrasound-assisted soaking treatment is mainly due to the formation of double helices by the linear segments of amylose within crystalline regions, resulting in a more efficient packing of the double helices. Compared with native and parboiled rice without ultrasound, ultrasound-assisted treatment increases the R1047/1022, indicating a highly ordered and compact granular structure Fig. 2B. Similar results were previously reported regarding the FTIR spectra (Ding et al., 2018).

3.5. XRD analysis

The X-ray diffraction spectra were analyzed, and the results were presented in Fig. 2C. It was observed that both native rice cultivars exhibited A-type crystalline patterns with main peaks at 15°, doublet at 17°, 18°, and 23° (Kraithong et al., 2018). Compared to Indica rice, Japonica rice had lower crystallinity due to its low amylose content (Cheetham & Tao 1998). After parboiling treatment, new minor peaks were observed at 12° and 20° (2θ), indicating a formation of V-type crystallinity, which was attributed to the retrogradation of amylose molecules (Tian et al., 2018). Ultrasound treatment facilitated the reorganization of amylose molecules within both the amorphous and crystalline region, contributing to the formation of a more stable and crystalline structure within the granules. (Cao & Gao 2020) reported that the ultrasound waves led to generate cavitations bubbles and then was subjected to rapid expansion and collapse. Ultrasound treatment could induce a cleavage of α-1, 6 glucosidic bonds within amylopectin and release linear glucans (Flores-Silva et al., 2017). These linear glucans tend to get self-associated, promoting a formation of V-type crystallinity. The crystalline regions exhibit a more compact and ordered arrangement compared to amorphous regions. Thus, in our study, the increased crystallinity suggested a higher stable structure present in ultrasound-assisted treated starch which decreased the availability and susceptibility of starch for enzymatic digestion.

3.6. Thermal properties

The thermal properties of rice, including "onset temperature (T$_o$)", "peak temperature (T$_p$)", "conclusion temperature (T$_c$)", and enthalpy change (ΔH), are presented in Table 2. It showed that Indica native rice exhibited an endothermic peak at around 80 °C, which was higher than that of Japonica rice due to the different crystalline and amylose contents (Fig. 2). When the ultrasound amplitude and time were applied, the melting peak gradually increased, representing internal changes in the intermolecular interactions (such as amylose/amylopectin and amylose/amylose chains) promoting the crystalline stability by reducing the starch chain flexibility in the amorphous regions. Thus, a high amount of thermal energy was required to disrupt the crystalline region during gelatinization. In addition, the ultrasound-assisted parboiled samples from Japonica rice cultivars exhibited notably lower ΔH (ranging from 1.14 to 4.86) values, while a slight increase in ΔH was seen at 15m30a, 30m30a, and 30m60a in Indica ultrasound-assisted parboiled rice. (Yang et al., 2019) reported that ΔH is the amount of energy per gram (dry matter), required to completely gelatinize the starch granules in the sample, suggesting more energy was required to
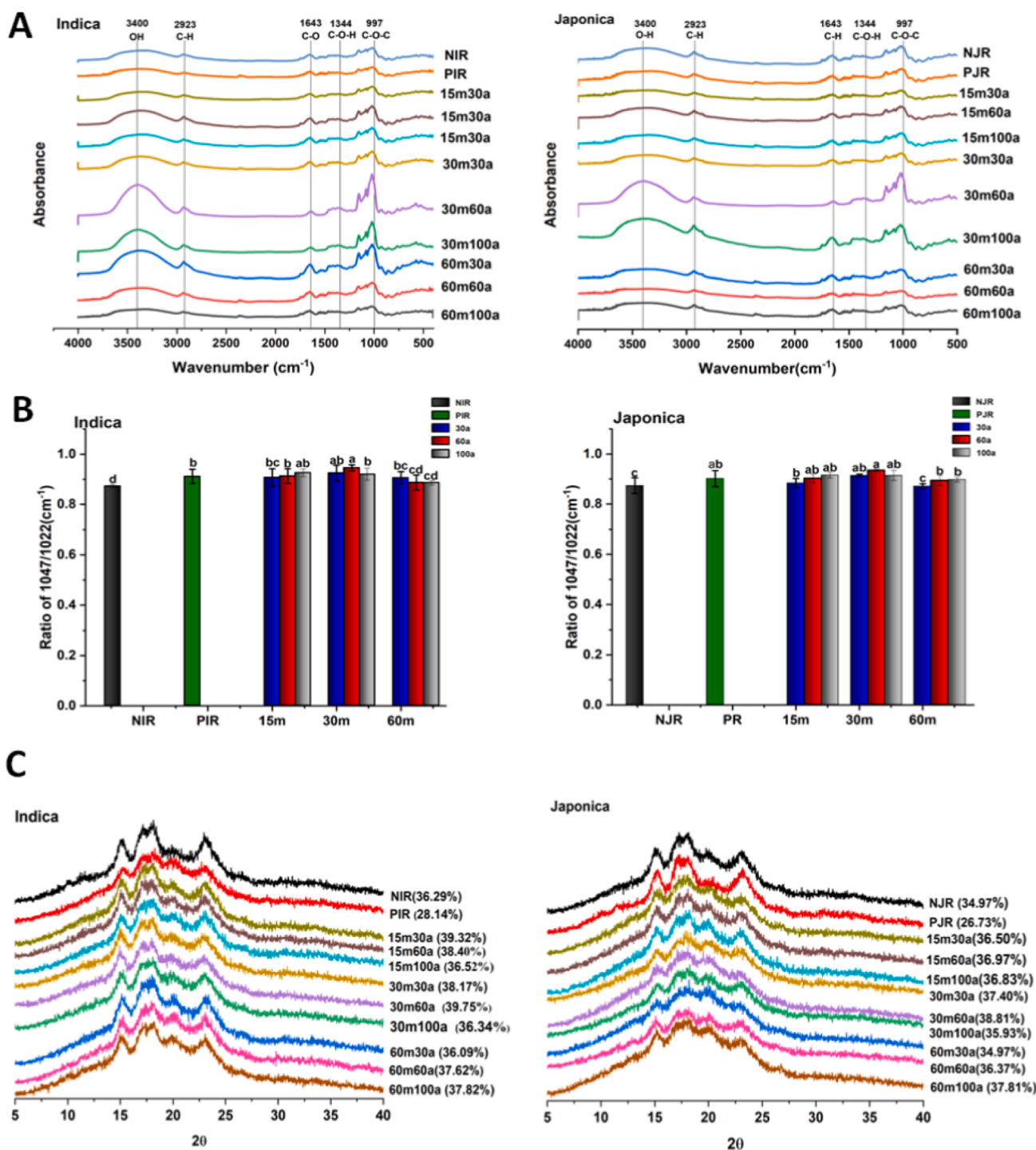
Fig. 2. FTIR spectra (A), short-range crystallinity (B) and X-ray diffraction pattern (C) of native, parboiled, and ultrasound-assisted parboiled Indica and Japonica rice cultivars. Values followed by the same lowercase letters of both rice cultivars do not differ significantly (p > 0.05). Bars represent standard deviations.

gelatinize Indica rice starch. In the present study, the increase in gelatinization temperature with ultrasound conditions was observed. (Biswas et al., 2020) have shown a linear association between the increasing content of amylose or resistant starch and gelatinization temperature. Starches comprising high amylose contents generally exhibit an increase in gelatinization temperature.

3.7. Pasting properties

Table 3 presents the viscosity parameters of each rice samples. Compare to the native raw rice, parboiled rice without ultrasonication displayed higher peak viscosity (PV), breakdown (BD), and lower setback values (SV), presenting less susceptibility to shear-thinning during cooking (Saleh et al., 2018). When subjected to ultrasound-assisted parboiling treatment, the peak and breakdown viscosities was further decreased with the processing time. During ultrasound-assisted

Table 2
Thermal properties of native, parboiled, and ultrasound-assisted parboiled Indica and Japonica rice cultivars.

Cultivars	Time (min)	Amplitude (%)	T_0 (°C)	T_p (°C)	T_c (°C)	ΔH(J/g)
Indica	NIR	0	74.67 ± 0.18[d]	80.31 ± 0.20[d]	87.15 ± 0.05[cd]	3.24 ± 0.26[a]
	PIR	0	72.4 ± 0.42[e]	81.2 ± 0.53[c]	89.51 ± 0.42[b]	3.37 ± 0.38[b]
	15	30	79.67 ± 0.06[a]	80.32 ± 0.46[d]	88.42 ± 0.70[bc]	3.74 ± 0.27[a]
		60	77.59 ± 0.01[b]	82.11 ± 0.29[b]	89.40 ± 0.63[b]	2.85 ± 0.13[ab]
		100	77.89 ± 0.21[b]	83.70 ± 0.15[a]	89.05 ± 0.54[b]	2.10 ± 0.04[b]
	30	30	76.21 ± 0.33[c]	82.35 ± 0.42[ab]	87.81 ± 0.23[c]	3.47 ± 0.18[a]
		60	78.08 ± 0.34[b]	81.14 ± 0.96[c]	88.67 ± 0.19[bc]	3.68 ± 0.34[a]
		100	76.16 ± 0.27[c]	81.44 ± 0.82[c]	87.56 ± 0.33[cd]	2.78 ± 0.22[ab]
	60	30	76.55 ± 0.40[c]	82.32 ± 0.52[ab]	87.56 ± 0.49[cd]	2.51 ± 0.49[b]
		60	78.88 ± 0.34[a]	83.34 ± 0.61[a]	91.29 ± 0.24[a]	2.82 ± 0.12[ab]
		100	78.04 ± 0.43[b]	83.39 ± 0.45[a]	89.32 ± 0.36[b]	2.39 ± 0.30[b]
Japonica	NJR	0	61.84 ± 0.15[f]	65.74 ± 0.11[d]	77.98 ± 0.13[b]	5.51 ± 0.23[a]
	PJR	0	62.19 ± 0.42[e]	68.63 ± 0.32[b]	75.43 ± 0.40[d]	2.57 ± 0.71[d]
	15	30	63.52 ± 0.21[d]	68.68 ± 0.19[b]	77.44 ± 0.01[b]	4.86 ± 0.08[b]
		60	63.22 ± 0.19[d]	67.72 ± 0.22[c]	76.61 ± 0.21[c]	3.64 ± 0.25[c]
		100	63.63 ± 0.30[d]	67.59 ± 0.30[c]	77.36 ± 0.16[b]	3.13 ± 0.42[c]
	30	30	64.42 ± 0.29[c]	67.51 ± 0.07[c]	77.64 ± 0.15[b]	3.55 ± 0.10[c]
		60	65.46 ± 0.31[b]	68.62 ± 0.48[b]	78.08 ± 0.38[a]	2.11 ± 0.17[d]
		100	64.12 ± 0.16[c]	67.55 ± 0.10[c]	76.04 ± 0.31[c]	2.48 ± 0.16[d]
	60	30	64.52 ± 0.30[c]	67.70 ± 0.26[c]	76.74 ± 0.22[c]	2.07 ± 0.05[d]
		60	65.34 ± 0.07[b]	69.18 ± 0.09[b]	75.72 ± 0.12[d]	2.20 ± 0.03[d]
		100	67.07 ± 0.06[a]	70.24 ± 0.15[a]	78.13 ± 0.22[a]	1.14 ± 0.02[e]

Values are means of triplicate determination ($p < 0.05$). To, onset temperature; Tp, peak temperature, Tc, conclusion temperature; ΔH, gelatinization enthalpy.

parboiling treatment, amylose undergoes retrogradation, promoting hydrogen bonds between starch molecules and rearranged starch crystalline structure. Amylose has a significant effect on breakdown viscosities (a measurement of cooked starch granules' susceptibility to become disintegrate) and a setback viscosity (re-crystallization measurement of gelatinized starch) (Li et al., 2021a). The lower peak and breakdown viscosity of ultrasound-assisted parboiled rice represents improved thermal stability, mechanical strength, and high interactions present between amylose molecules to create a more stable starch structure.

3.8. In vitro digestion

Resistant starch of each rice cultivar is presented in Table 1. Compared with Japonica rice, Indica is rich in crystallinity and shows strong resistance to digestion manifested by higher RS (18.98) and lower eGI (57.60) as shown in Fig. 3. The resistance to digestion was further

increased by ultrasound-assisted parboiling treatment for example, when rice was subjected to 30 min of ultrasound at the amplitude of 60%, it increased from 16.98 to 27.41 and 7.32 to 18.04 for Indica and Japonica rice respectively. It was reported that the digestibility of starch was affected by granule morphology and amylopectin structure (Sopawong et al., 2022). In the present study, the lower level of GI could be assigned to the formation of fresh newly formed amylose crystalline structure during parboiling. Ultrasound induced the reorganization of disrupted starch molecules, whereby fragmented chains are realigned with the amorphous region of the amylopectin chains. Generally, crystalline regions exhibited a more compact and ordered arrangement compared to amorphous regions (Flores-Silva et al., 2017). This reorganization of starch molecules within the granules imposed limitations on enzymatic hydrolysis, resulting in a decelerated digestion process (Khurshida et al., 2021).

3.9. Texture profile analysis (TPA)

Rice textural properties of each sample were presented in Supplementary Table 4. Hardness refers to the texture or consistency of a substance, typically refers to the firmness or softness of rice kernels and has great influence on cooked rice palatability (Park et al., 2020). When compared with Japonica, the Indica rice hardness was higher ($p < 0.05$). This finding is consistent with (Kang et al., 2006), who concluded that the decreased hardness observed in Japonica rice can be attributed to the interplay between amylopectin structure, amylose content, and protein content. Meanwhile, ultrasound treated parboiled sample showed a significantly softer rice texture, which is consistent with (Park & Han 2016). Japonica rice has a lower hardness than Indica, and it further decreased from 1766.95 to 1240.22 and from 2655.16 to 1890.08 for 30 min of ultrasound with 30% amplitude, respectively. The decrease in hardness observed after ultrasound treatment may be attributed to the high pressure gradients and high local velocities produced by ultrasound. This result in the formation of cracks and fissures, facilitating the penetration of water into the interior of the rice grains during cooking. As a result, the hardness of the cooked rice decreased. The cracks caused by ultrasound resulted in rupture and amylose leaching. The leached components could increase adhesiveness (Zhang et al., 2015). The decrease in hardness of cooked rice was directly correlated to chewiness, as it indicates that less force or energy is required to bite and chew the rice grains. The rice springiness is related to the extension of rice grains against the contact surface as they have pulled away (teeth). While the gumminess relies on the energy required for the disintegration of rice for the swallowing stage. Ultrasound treated parboiled rice grains exhibited lower gumminess for both rice cultivars. Therefore, ultrasound-assisted parboiled rice showed significantly lower chewiness than native or parboiled rice without ultrasound treatment.

4. Conclusion

The present study suggested that ultrasound-assisted parboiling treatment promoted a more ordered and compact granular structure. The newly organized structure exhibited characteristics of a V-type crystal arrangement as indicated by changes in the crystallinity. It enhanced the overall smoothness of the rice morphology, suggesting a potential mechanism for improved resistance to digestion. It developed a formation of amylose chains and decreased the enzyme penetration into the granules, thus facilitating higher RS content and lower glycemic index. These changes contributed to the potential health benefits, especially for diabetic patients and consumer preference for parboiled rice produced with ultrasound treatment during soaking.

CRediT authorship contribution statement

Alia Shah: Investigation, Formal analysis, Writing – original draft.

Table 3
Pasting properties of native, parboiled, and ultrasound-assisted parboiled Indica and Japonica rice cultivars.

Cultivars	Time (min)	Amplitude (%)	PV/cp	BD/cp	FV/cp	SV/cp
Indica	NIR	0	1081.67 ± 0.57^b	527.66 ± 0.57^a	$1324.45 \pm 0.27^{\ h}$	$242.42 \pm 0.15^{\ j}$
	PIR	0	1131.52 ± 0.74^a	539.16 ± 0.82^a	1294.24 ± 0.62^i	$221.53 \pm 0.41^{\ k}$
	15	30	$741.41 \pm 0.92^{\ g}$	126.33 ± 0.57^d	$1420.49 \pm 0.20^{\ g}$	680.51 ± 0.38^i
		60	783.13 ± 0.42^f	$47.8 \pm 0.34^{\ g}$	1630.29 ± 0.27^e	880.41 ± 0.28^d
		100	787.75 ± 0.49^f	$48.16 \pm 0.20^{\ g}$	1741.60 ± 0.26^c	953.56 ± 0.35^b
	30	30	881.70 ± 0.56^e	158.13 ± 1.10^c	1628.48 ± 0.59^e	$748.46 \pm 0.15^{\ h}$
		60	943.85 ± 0.35^c	54.52 ± 0.53^f	1926.24 ± 0.20^b	1146.44 ± 0.29^a
		100	1038.75 ± 0.49^b	197.93 ± 0.60^b	1956.45 ± 0.31^a	918.30 ± 0.00^c
	60	30	898.45 ± 0.77^d	156.76 ± 0.92^c	$1728.28 \pm.023^c$	830.33 ± 0.22^f
		60	$668.80 \pm 0.28^{\ h}$	$40.26 \pm 0.76^{\ h}$	1430.53 ± 0.11^f	$762.32 \pm 0.32^{\ g}$
		100	881.70 ± 0.56^e	105.26 ± 0.70^e	1714.15 ± 0.13^d	858.61 ± 0.53^e
Japonica	NJR	0	1152.40 ± 0.10^c	703.90 ± 0.60^b	1290.76 ± 0.40^i	$138.53 \pm 0.58^{\ h}$
	PJR	0	1237.31 ± 0.42^b	718.11 ± 0.94^a	1226.13 ± 0.71^j	$131.92 \pm 0.71^{\ h}$
	15	30	904.89 ± 0.53^f	$114.60 \pm 1.51^{\ g}$	1830.53 ± 0.51^b	924.55 ± 0.46^a
		60	1060.85 ± 0.73^d	254.10 ± 1.00^d	1910.63 ± 0.83^a	850.76 ± 0.36^c
		100	1060.50 ± 0.87^d	294.90 ± 0.87^c	1793.83 ± 0.64^c	735.50 ± 1.03^e
	30	30	$754.90 \pm 0.43^{\ h}$	44.03 ± 0.37^i	1684.63 ± 0.51^f	930.77 ± 0.56^a
		60	$890.46 \pm 0.54^{\ g}$	124.56 ± 0.85^f	1778.20 ± 0.10^d	888.54 ± 0.82^b
		100	1040.48 ± 0.24^e	308.16 ± 0.90^c	1680.73 ± 0.68^f	$640.19 \pm 0.01^{\ g}$
	60	30	738.50 ± 0.62^i	$65.26 \pm 0.85^{\ h}$	$1538.56 \pm 0.56^{\ g}$	800.20 ± 0.10^d
		60	1394.70 ± 0.45^a	242.20 ± 0.19^e	1740.66 ± 0.55^e	676.26 ± 0.15^f
		100	1064.57 ± 0.22^d	700.93 ± 0.58^b	$1452.80 \pm 0.60^{\ h}$	58.22 ± 0.06^i

Data values are means $\pm$ standard deviation followed by the different letters in the same column indicating a significant difference ($p < 0.05$). PV, peak viscosity; BD, breakdown, FV, final viscosity; SV, setback viscosity.
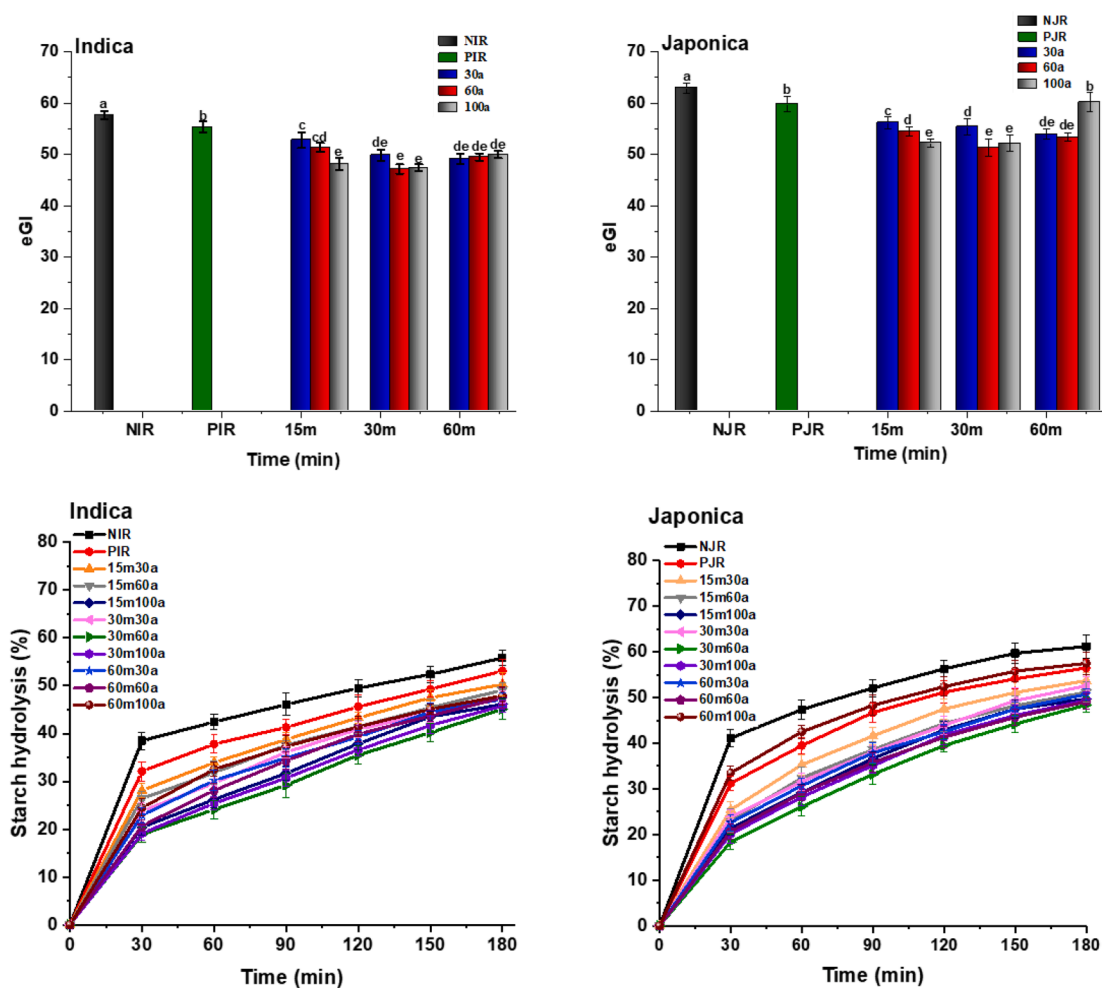

Fig. 3. The quantification of the expected glycemic index (eGI) and hydrolysis curve of native, parboiled, and ultrasound-assisted parboiled Indica and Japonica rice cultivars. Values followed by the same uppercase letters are not significantly different ($p > 0.05$). Bars represent standard deviations.

Yunchun Wang: Methodology, Data curation. **Han Tao:** Writing – review & editing. **Wencheng Zhang:** Funding acquisition. **Shuqing Cao:** Supervision, Project administration.

Declaration of Competing Interest

The authors declare that they have no known competing financial interests or personal relationships that could have appeared to influence the work reported in this paper.

Data availability

Data will be made available on request.

Appendix A. Supplementary material

Supplementary data to this article can be found online at https://doi.org/10.1016/j.fochx.2023.100816.

References

AOAC (2002). AOAC Official Method 2001.11 (2002). Protein (crude) in animal feed, forage (plant.pdf). *AOAC INTERNATIONAL*.

Biswas, P., Das, M., Boral, S., Mukherjee, G., Chaudhury, K., & Banerjee, R. (2020). Enzyme mediated resistant starch production from Indian Fox Nut (Euryale ferox) and studies on digestibility and functional properties. *Carbohydrate Polymers, 237*, Article 116158.

Cai, C., Tian, Y., Yu, Z., Sun, C., & Jin, Z. (2020). In vitro digestibility and predicted glycemic index of chemically modified rice starch by one-step reactive extrusion. *Starch-Stärke, 72*, Article 1900012.

Cao, M., & Gao, Q. (2020). Effect of dual modification with ultrasonic and electric field on potato starch. *International Journal of Biological Macromolecules, 150*, 637–643.

Cheetham, N. W., & Tao, L. (1998). Variation in crystalline type with amylose content in maize starch granules: An X-ray powder diffraction study. *Carbohydrate Polymers, 36*, 277–284.

Ding, J., Hou, G. G., Dong, M., Xiong, S., Zhao, S., & Feng, H. (2018). Physicochemical properties of germinated dehulled rice flour and energy requirement in germination as affected by ultrasound treatment. *Ultrasonics Sonochemistry, 41*, 484–491.

Englyst, H. N., Kingman, S., & Cummings, J. H. (1992). Classification and measurement of nutritionally important starch fractions. *European Journal of Clinical Nutrition, 46*, S33–S50.

Estivi, L., Brandolini, A., Condezo-Hoyos, L., & Hidalgo, A. (2022). Impact of low-frequency ultrasound technology on physical, chemical and technological properties of cereals and pseudocereals. *Ultrasonics Sonochemistry, 86*, Article 106044.

Flores-Silva, P. C., Roldan-Cruz, C. A., Chavez-Esquivel, G., Vernon-Carter, E. J., Bello-Perez, L. A., & Alvarez-Ramirez, J. (2017). In vitro digestibility of ultrasound-treated corn starch. *Starch-Stärke, 69*, 1700040.

Goñi, I., Garcia-Alonso, A., & Saura-Calixto, F. (1997). A starch hydrolysis procedure to estimate glycemic index. *Nutrition Research, 17*, 427–437.

Gui, Y., Wei, X., Yang, N., Guo, L., Cui, B., Zou, F., Lu, L., Liu, P., & Fang, Y. (2022). Comparison of structural and functional properties of maize starch produced with commercial or endogenous enzymes. *International Journal of Biological Macromolecules, 209*, 2213–2225.

Kang, H.-J., Hwang, I.-K., Kim, K.-S., & Choi, H.-C. (2006). Comparison of the physicochemical properties and ultrastructure of japonica and indica rice grains. *Journal of Agricultural and Food Chemistry, 54*, 4833–4838.

Kaur, H., & Gill, B. S. (2019). Effect of high-intensity ultrasound treatment on nutritional, rheological and structural properties of starches obtained from different cereals. *International Journal of Biological Macromolecules, 126*, 367–375.

Kentish, S., & Feng, H. (2014). Applications of power ultrasound in food processing. *Annual Review of Food Science and Technology, 5*, 263–284.

Khurshida, S., Das, M. J., Deka, S. C., & Sit, N. (2021). Effect of dual modification sequence on physicochemical, pasting, rheological and digestibility properties of cassava starch modified by acetic acid and ultrasound. *International Journal of Biological Macromolecules, 188*, 649–656.

Kraithong, S., Lee, S., & Rawdkuen, S. (2018). Physicochemical and functional properties of Thai organic rice flour. *Journal of Cereal Science, 79*, 259–266.

Kunyanee, K., & Luangsakul, N. (2020). The effects of ultrasound–assisted recrystallization followed by chilling to produce the lower glycemic index of rice with different amylose content. *Food Chemistry, 323*, Article 126843.

Lamberts, L., Rombouts, I., Brijs, K., Gebruers, K., & Delcour, J. A. (2008). Impact of parboiling conditions on Maillard precursors and indicators in long-grain rice cultivars. *Food Chemistry, 110*, 916–922.

Li, H., Yan, S., Yang, L., Xu, M., Ji, J., Mao, H., Song, Y., Wang, J., & Sun, B. (2021a). Starch gelatinization in the surface layer of rice grains is crucial in reducing the stickiness of parboiled rice. *Food Chemistry, 341*, Article 128202.

Li, M., Li, J., & Zhu, C. (2018). Effect of ultrasound pretreatment on enzymolysis and physicochemical properties of corn starch. *International Journal of Biological Macromolecules, 111*, 848–856.

Li, S., Zhang, R., Lei, D., Huang, Y., Cheng, S., Zhu, Z., Wu, Z., & Cravotto, G. (2021b). Impact of ultrasound, microwaves and high-pressure processing on food components and their interactions. *Trends in Food Science and Technology, 109*, 1–15.

Liang, Q., Chen, X., Ren, X., Yang, X., Raza, H., & Ma, H. (2021). Effects of ultrasound-assisted enzymolysis on the physicochemical properties and structure of arrowhead-derived resistant starch. *Lwt, 147*, Article 111616.

Liu, G., Gu, Z., Hong, Y., Wei, H., Zhang, C., Huang, S., Chen, Y., Lu, Y., & Li, Y. (2020). Effects of molecular interactions in debranched high amylose starch on digestibility and hydrogel properties. *Food Hydrocolloids, 101*, Article 105498.

Lu, Z.-H., Belanger, N., Donner, E., & Liu, Q. (2018). Debranching of pea starch using pullulanase and ultrasonication synergistically to enhance slowly digestible and resistant starch. *Food Chemistry, 268*, 533–541.

Morales-Trejo, F., Trujillo-Ramírez, D., Aguirre-Mandujano, E., Lobato-Calleros, C., Vernon-Carter, E. J., & Alvarez-Ramirez, J. (2022). Ultrasound-Assisted Extraction of Lychee (Litchi chinensis Sonn.) Seed Starch: Physicochemical and Functional Properties. *Starch-Stärke, 74*, 2100092.

Nie, H., Li, C., Liu, P.-H., Lei, C.-Y., & Li, J.-B. (2019). Retrogradation, gel texture properties, intrinsic viscosity and degradation mechanism of potato starch paste under ultrasonic irradiation. *Food Hydrocolloids, 95*, 590–600.

Pal, P., Singh, N., Kaur, P., & Kaur, A. (2018). Effect of parboiling on phenolic, protein, and pasting properties of rice from different paddy varieties. *Journal of Food Science, 83*, 2761–2771.

Park, D.-J., & Han, J.-A. (2016). Quality controlling of brown rice by ultrasound treatment and its effect on isolated starch. *Carbohydrate Polymers, 137*, 30–38.

Park, J.-W., Lee, S., Yoo, B., & Nam, K. (2020). Effects of texture properties of semi-solid food on the sensory test for pharyngeal swallowing effort in the older adults. *BMC Geriatrics, 20*, 1–5.

Peng, Y., Mao, B., Zhang, C., Shao, Y., Wu, T., Hu, L., Hu, Y., Tang, L., Li, Y., & Tang, W. (2021). Influence of physicochemical properties and starch fine structure on the eating quality of hybrid rice with similar apparent amylose content. *Food Chemistry, 353*, Article 129461.

Saleh, M., Akash, M., & Ondier, G. (2018). Effects of temperature and soaking durations on the hydration kinetics of hybrid and pureline parboiled brown rice cultivars. *Journal of Food Measurement and Characterization, 12*, 1369–1377.

Sittipod, S., & Shi, Y.-C. (2016). Changes in physicochemical properties of rice starch during steeping in the parboiling process. *Journal of Cereal Science, 69*, 398–405.

Sopawong, P., Warodomwichit, D., Srichamnong, W., Methacanon, P., & Tangsuphoom, N. (2022). Effect of physical and enzymatic modifications on composition, properties and in vitro starch digestibility of Sacred Lotus (Nelumbo nucifera) seed flour. *Food, 11*, 2473.

Sowbhagya, C., & Bhattacharya, K. (2001). Changes in pasting behaviour of rice during ageing. *Journal of Cereal Science, 34*, 115–124.

Tao, H., Lu, F., Zhu, X.-F., Xu, G.-X., Xie, H.-Q., Xu, X.-M., & Wang, H.-L. (2021). Removing surface proteins promote the retrogradation of wheat starch. *Food Hydrocolloids, 113*, Article 106437.

Thammapat, P., Meeso, N., & Siriamornpun, S. (2016). Effects of the traditional method and an alternative parboiling process on the fatty acids, vitamin E, γ-oryzanol and phenolic acids of glutinous rice. *Food Chemistry, 194*, 230–236.

Tian, J., Cai, Y., Qin, W., Matsushita, Y., Ye, X., & Ogawa, Y. (2018). Parboiling reduced the crystallinity and in vitro digestibility of non-waxy short grain rice. *Food Chemistry, 257*, 23–28.

Vela, A. J., Villanueva, M., Solaesa, Á. G., & Ronda, F. (2021). Impact of high-intensity ultrasound waves on structural, functional, thermal and rheological properties of rice flour and its biopolymers structural features. *Food Hydrocolloids, 113*, Article 106480.

Venn, B., & Green, T. J. (2007). Glycemic index and glycemic load: measurement issues and their effect on diet–disease relationships. *European Journal Clinical Nutrition, 61*, S122–S131.

Yang, D., Gao, S., & Yang, H. (2020). Effects of sucrose addition on the rheology and structure of iota-carrageenan. *Food Hydrocolloids, 99*, Article 105317.

Yang, W., Kong, X., Zheng, Y., Sun, W., Chen, S., Liu, D., Zhang, H., Fang, H., Tian, J., & Ye, X. (2019). Controlled ultrasound treatments modify the morphology and physical properties of rice starch rather than the fine structure. *Ultrasonics Sonochemistry, 59*, Article 104709.

Zhang, X., Wang, L., Cheng, M., Wang, R., Luo, X., & Li, Y. (2015). Influence of ultrasonic enzyme treatment on the cooking and eating quality of brown rice. *Journal of Cereal Science, 63*, 140–146.

Zhang, Y., Zhang, Y., Li, B., Wang, X., Xu, F., & Zhu, K. (2019). In vitro hydrolysis and estimated glycemic index of jackfruit seed starch prepared by improved extrusion

cooking technology. *International Journal of Biological Macromolecules, 121,* 1109–1117.

Zia-ud-Din, Xiong, H., & Fei, P. (2017). Physical and chemical modification of starches: A review. *Critical Reviews in Food Science and Nutrition, 57,* 2691–2705.

Zou, J., Xu, M., Tang, W., Wen, L., & Yang, B. (2020). Modification of structural, physicochemical and digestive properties of normal maize starch by thermal treatment. *Food Chemistry, 309,* Article 125733.